INTERNATIONAL SCIENTIFIC AND VOCATIONAL JOURNAL (ISVOS JOURNAL)

Vol.: 3 Issue: 1 Date: June 2019 Received: 26.12.2018 Accepted: 5.3.2019 Final Version: 1.06.2019

ISVOS Journal, 2019, 3(1): 1-7

Bismuth Telluride (Bi_2Te_3) Nanostructure for Thermoelectric Applications

Mohammad Ruhul Amin Bhuiyan[a], Hayati Mamur[b,1]

[a]Islamic University, Faculty of Engineering and Technology, Electrical and Electronic Engineering, 7003, Kushtia, Bangladesh
[b]Manisa Celal Bayar University, Faculty of Engineering, Electrical and Electronics Engineering, 45140, Manisa, Turkey

Abstract

The bismuth telluride (Bi_2Te_3) nanostructure is the most commonly used in thermoelectric (TE) applications. The different processes are utilized to produce the Bi_2Te_3 nanostructure. Herein, the used process is an efficient and cost effective two-step co-precipitation chemical solution route. The process has been formed by dissolving the bismuth (III) nitrate pentahydrate, $Bi(NO_3)_3.5H_2O$ and tellurium dioxide, TeO_2 into the same inorganic nitric acid, HNO3 with the two-step co-precipitation of sodium hydroxide, NaOH and sodium borohydride, HNaB4. The characterizing tools such as x-ray diffraction (XRD), ultraviolet absorbance (UV), fourier transform infrared spectrometry (FTIR), scanning electron microscopy (SEM), energy dispersive analysis of x-ray (EDAX), atomic force microscopy (AFM), and transmission electron microscopy (TEM) were employed to produce the Bi_2Te_3 powders. According to these results, the obtained powders have been confirmed as a nanostructure form of about low dimension that can be easily used in TE applications.

Keywords: "Bismuth telluride (Bi_2Te_3); Nanostructures; Chemical solution route; Structural and microstructural characterization; Optical characterization"

1. Introduction

The Bi_2Te_3 semiconductors are widely used in thermoelectric modules (TEMs). The TEMs have been the subject of many studies since these TEMs provide an increased efficiency. They convert thermal energy into electrical energy directly. They are environmentally friendly, because they are made of semiconductor and work quietly and have a long life [1].

A great number of thermoelectric (TE) materials have been developed with improved the TE properties to utilize its applications. The Bi_2Te_3 is one of the most commonly used for TE applications. The manufacture of TEMs that could reach a theoretical efficiency is not a trivial pursuit. Therefore, it requires a huge development to research infrastructure. Ultra–fine device quality material needs the concern efforts involving physicists, chemists, electronics, and material researchers.

To produce the Bi_2Te_3 nanostructure, many researchers have employed the different process. Khade et al. [2] used a mechanical alloying method to obtain the Bi_2Te_3 nanostructure. Bi_2Te_3 thin films were studied by Sudarshan et al [3] in view of electrical and thermal properties in thermal evaporation. A novel route to nanostructured Bi_2Te_3 films was developed by using of an electrodeposition method by Burton et al [4]. Some a lithographic, a pulsed laser ablation, an electrochemical, a spark plasma sintering, a chemical solution methods also used some different studies [5–12]. By means of these applications and experiments, the chemical solution process is the very important synthesis process because supplied plenty of promising process for developing the nanostructures with regard to financial aspect and possible to mass-production of nanostructures. The capability to mass develop nanostructure materials is essential to the TE nanostructure research. Among of these methods, the chemical solution synthesis method is satisfactory accesses for developing these nanostructures with agreeable efficiency. Ultimately, the synthesis method and the aggregation of Bi_2Te_3 inflexible nanoforms has been a great number change for enabling the mass-production of efficient and quality devices for TEM practices [13–15].

The chemical solution process, a great amount of nanostructure TE materials like Bi_2Te_3 and its alloy have been profitably produced with different morphologies of nano size particles like as nanoflakes, nanorods, nanotubes and so on [16–20]. These alloys would be the considerable for ongoing nano composite TE exploration. A few derivative utilization like as nanoplating and nanocoating process has also been improved by using the chemical solution process. Some chemical solution techniques are efficient and miscellaneous processes for manufacturing these nanosize materials and appropriate for these TEM applications. In

[1] Corresponding Author. Tel.: +90-236-201-2163; fax: +90-236-241-2143.
E-mail: hayati.mamur@cbu.edu.tr

this paper, a cost-effective chemical solution process has been demonstrated according to authors' review papers for producing the device quality Bi_2Te_3 nanoform powder for TEM applications [21, 22].

2. Material and Methods

In this study, these materials in Table 1 were used in order to carry out the process. Firstly, the reagents of $Bi(NO_3)_3.5H_2O$ and TeO_2 were taken. These were used as initialization materials for the co–precipitation of an ordinary process. Secondly, the solvents of HNO_3, NaOH, $NaBH_4$ and Ethanol were accumulated. These solvents were also applied without any further purification.

Just before of the obtaining of Bi_2Te_3 nanostructure, $Bi(NO_3)_3.5H_2O$ and TeO_2 were made use of as a precursor in this process. The precursor were included in the solution with stoichiometric ratio of Bi:Te (2:3) for the co–precipitation. Moreover, NaOH solution was handled for a precipitation of $BiONO_3$ and TeO_2. Then the solution was organized the pH value of the solution. Furthermore, $NaBH_4$ was operated as a reducing agent for removing the oxidization.

Table 1. These materials for process.

Materials	Purity criteria	Purpose	Company
$Bi(NO_3)_3.5H_2O$	≥98%	co–precipitation	Sigma–Aldrich
TeO_2	≥97%	co–precipitation	Sigma–Aldrich
HNO_3	~70 %	solvent	Sigma–Aldrich
NaOH	98–100%	solvent	Sigma–Aldrich
$NaBH_4$	98–100%	solvent	Mark
Ethanol	Analytical grade	solvent	Mark
H	99%	oxidization	-

For preparing these samples, the experimental and measurement methods are handled in details in authors' previous report [9]. The obtained samples contained a little oxide. The hydrogen (H) gas was passed as a solution for this oxidation. For this, a computer controlled treatment with 99% at ~250°C pure hydrogen gas was used. The oxidation of the samples obtained by passing this hydrogen gas is reduced to a very low level. For preparing these solutions, the reagents of $Bi(NO_3)_3.5H_2O$ and TeO_2 easily dissolve in HNO_3.

The carried out chemical reaction is given as follows:

$$Bi(NO_3)_3.5H_2O\ (heat \sim 70^o\ to\ 80^oC) \rightarrow 3H_2O + 2HNO_3 + BiNO_3(OH)_2$$

$$2TeO_2 + HNO_3 \rightarrow Te_2(NO_3)O_3(OH)$$

$$NaOH + HNO_3 \rightarrow NaNO_3 + H_2O$$

$$2Bi_2O_3 + 9TeO_3 + 6NaBH_4 \rightarrow 2Bi_2Te_3 + 3NaTeO_3 + 6H_2BO_3 + 6H_2O$$

Consequently, the black colour Bi_2Te_3 nanostructure form was synthesised.

3. Results and Discussion

The chemical solution route is quite suitable way for Bi_2Te_3 nanoscale thermoelectric production. Figure 1 indicates the XRD spectra of Bi_2Te_3 nanopowders.

The main reflections are quite well indexed to the reference code. Evidently, sample 2 all the diffraction peaks could be indexed to pure rhombohedra Bi_2Te_3 nanostructure, which is reference code 98–018–4631 which provide XRD machine for Bi_2Te_3 powder diffraction standards data same as JCPDS. The spectrum indicating the phase purity of the Bi_2Te_3 nanopowders. It shows that the structure indicate the nanostructure with a (015) identified orientation (peak having sharp and higher intensity). In order to compare the spectrum with the Bi_2Te_3 nanostructure standard reference code, corresponding to the diffraction spectra belonged to diffraction planes of (015), (1010), (110) (205), (0210), (1115), (125) and (2110) of Bi_2Te_3 were exhibited with other researcher reports [23, 24].

The absorption spectra of Bi_2Te_3 nanostructures have been analyzed at room temperature using a UV-vis spectrophotometer as predicted in figure 2. It can be seen that the absorption spectra of the Bi_2Te_3 nanostructures were observed peaks for the samples between 200 and 240 nm.

The optical band gap or energy of the band gap is defined for all samples utilizing Tauc's equation, $\alpha h\nu = A(h\nu - Eg)^n$ [25,26]. Where n is equal to 2 and 1/2 for direct and indirect transitions respectively, α is the absorption coefficient. A is an energy independent constant. The variations of $(\alpha h\nu)^2$ with E (hν) for different Bi_2Te_3 samples and with the extrapolation of the straight line to intersect with the E-axis are indicate the band gap value. It can be seen that the direct band gap in these materials resulting from electronic transitions, which means these materials involve only the electrons between the valance and the conduction bands without any interaction with the lattice [27]. It was revealed a large blue shift from the standard bulk Bi_2Te_3 band gap (Eg = 0.15 eV) [28] due to the nano-size effect. The dependency of the band gap energy Eg on the particle size arises from the overlapping of orbitals and energy levels of atoms and molecules in the particle. In the nano-particle where there is a few number of atoms and molecules, the number of overlapped energy levels are small. So, the width of each of the conduction and valance bands are narrow. This will cause an increase in energy gap between the valance and conduction bands.

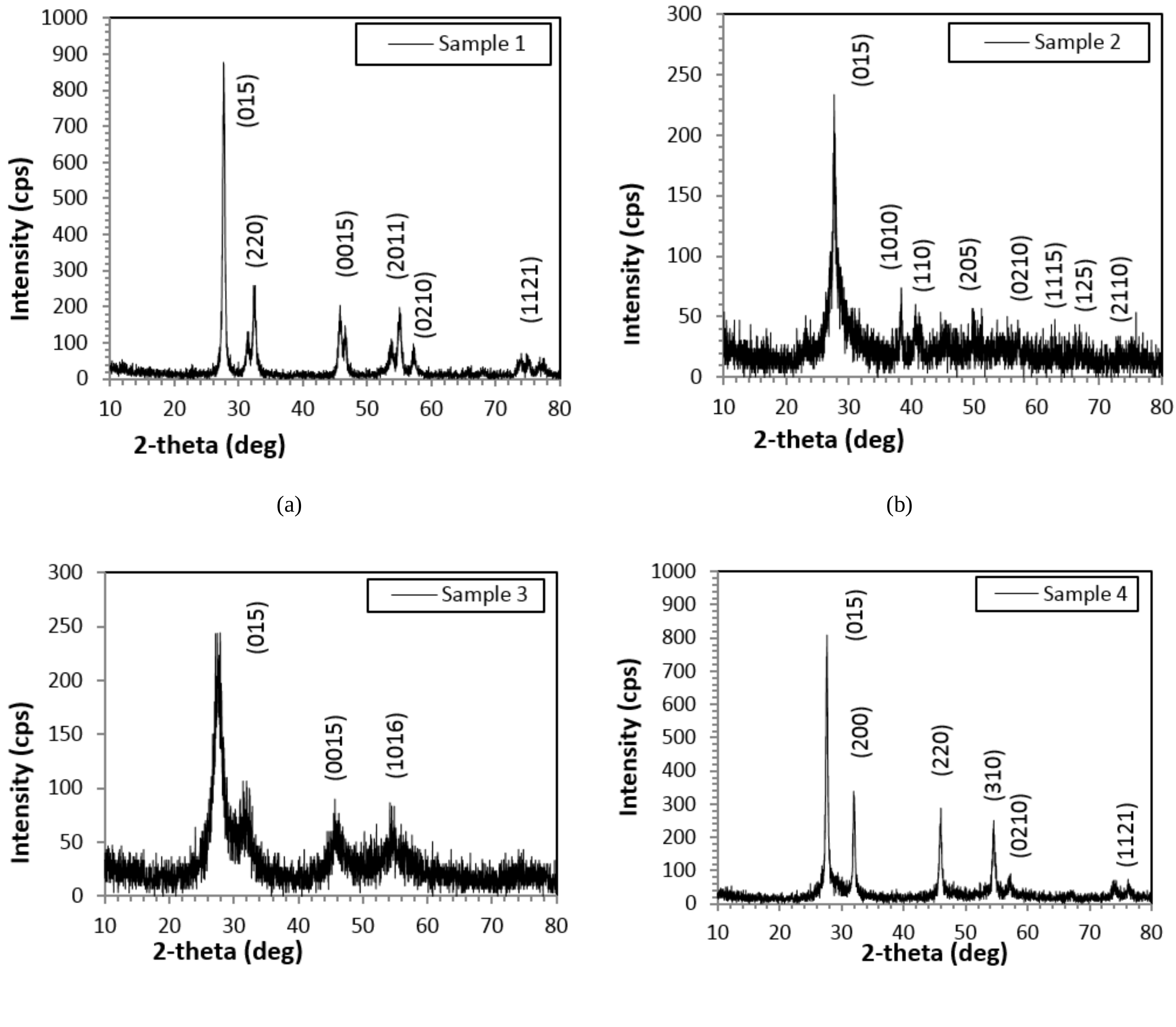

Figure 1. XRD spectra of Bi_2Te_3 nanostructures.

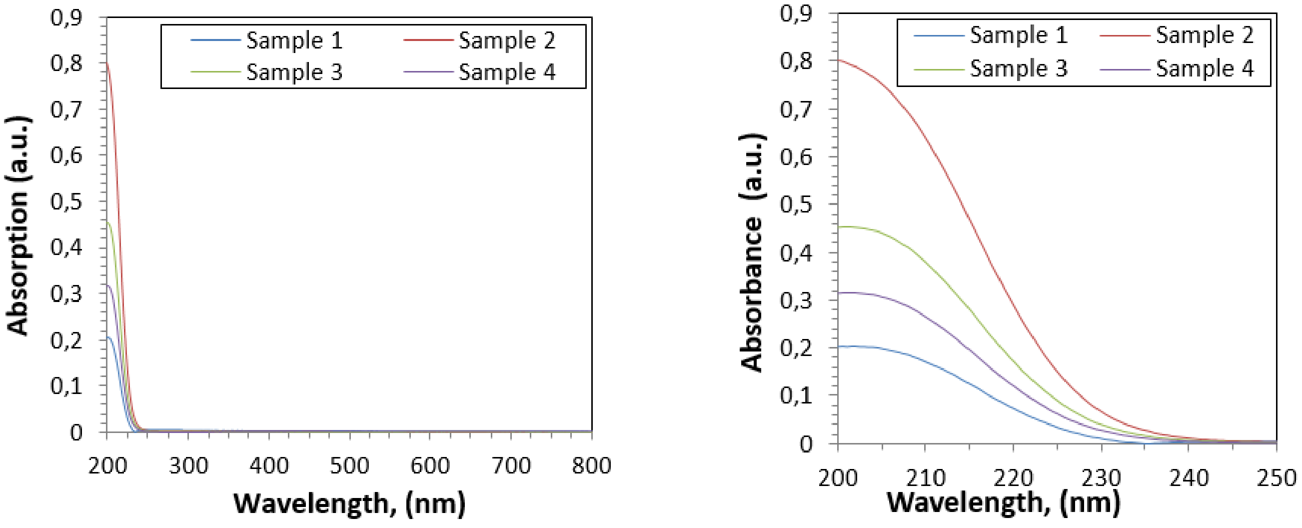

(a) UV Spectra (b) Simplified UV spectra

Figure 2. UV spectra of Bi_2Te_3 nanostructure.

Figure 3 demonstrates the FTIR transmittance spectra of Bi_2Te_3 nanostructure for the inspected samples in the study. According to the literature report [29] , the expected peak for the FTIR spectra of Bi_2Te_3 nanostructure are absorbed CO_2, at 1014 cm^{-1} belongs to Bi, at 1115 cm^{-1} corresponds to the C–O bond, at 1400 cm^{-1} corresponds to the O–H bond, at 1700 cm^{-1} corresponds to the C=O bond and two weak peaks at about 2924 cm^{-1} and 2853 cm^{-1} to the C–H bond of the $–CH_3$ and $–CH_2–$ groups. In examined sample 2 in the study, the peaks 949.47 cm^{-1}, 1265.85 cm^{-1}, 1392.75 cm^{-1}, 2662.93 cm^{-1} and 2976.97 cm^{-1} were observed. They were the similar nature to Bi, C–O, O–H, C–H bond and other.

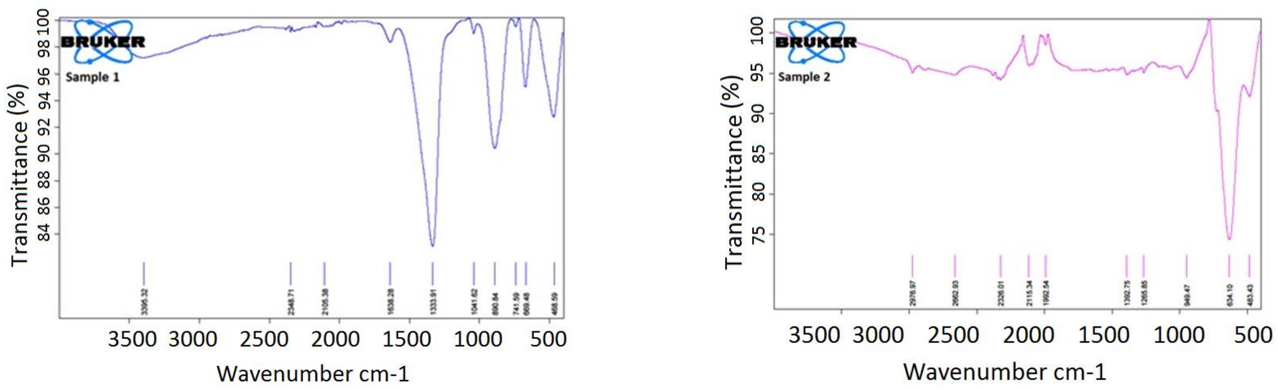

(a) (b)

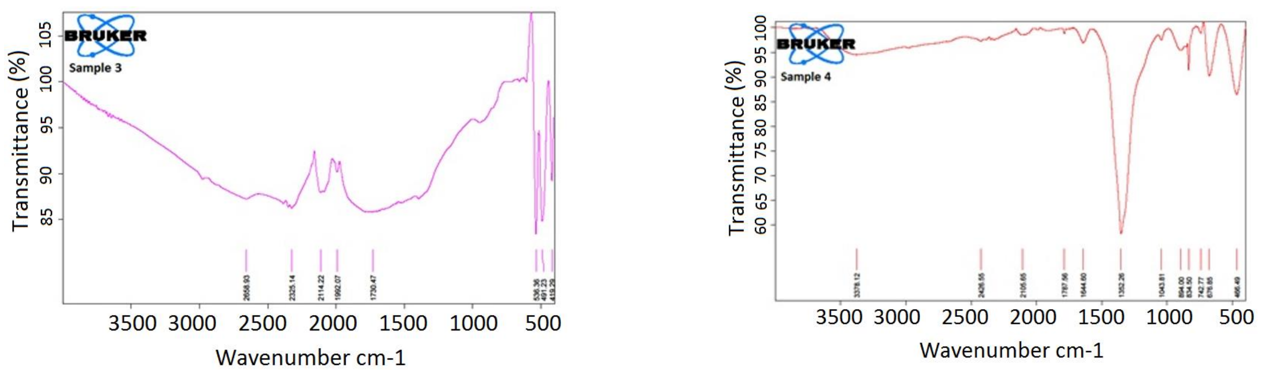

(c) (d)

Figure 3. FTIR spectra of Bi_2Te_3 nanopowders.

According to obtained data, these results illustrated, the prepared samples show that the sample 2 is the optimum level for pure Bi_2Te_3 nanopowders production. After finishing these characterization, SEM, EDX, AFM and TEM were studied only the sample 2. Figure 4(a) shows the SEM image of Bi_2Te_3 nanostructure that reveals the sample was arranged sequentially and agglomerated. It exhibit quasi spherical granule shapes in agglomerated clusters and the grain dimensions are small in nanometer range according to the other researcher reports [30]. Experimental results suggest that the behaviour is related to grain boundaries which shows a stacking of low dimentional particles. Notably influence the TE properties of this nanostructuration involve a bounding surface boundaries that are impeachable for broad phonon scattering circumstance. These results propose that the Bi_2Te_3 can be a good aspirant for low temperature range of TE applications. Figure 4(b) shows the EDAX spectrum that materials of Bi and Te were organized with their atomic stoichiometric ratio. The atomic composition of Bi and Te elements is approximately 2:3 within an instrumental accuracy, confirming that the nanostructure is composed of only Bi and Te. The significant increase of around an order of magnitude in figure of merit at low temperature compared to the stoichiometric sample. Due to its stoichiometric behaviour the Bi_2Te_3 is one of the promising candidates for TE applications [31].

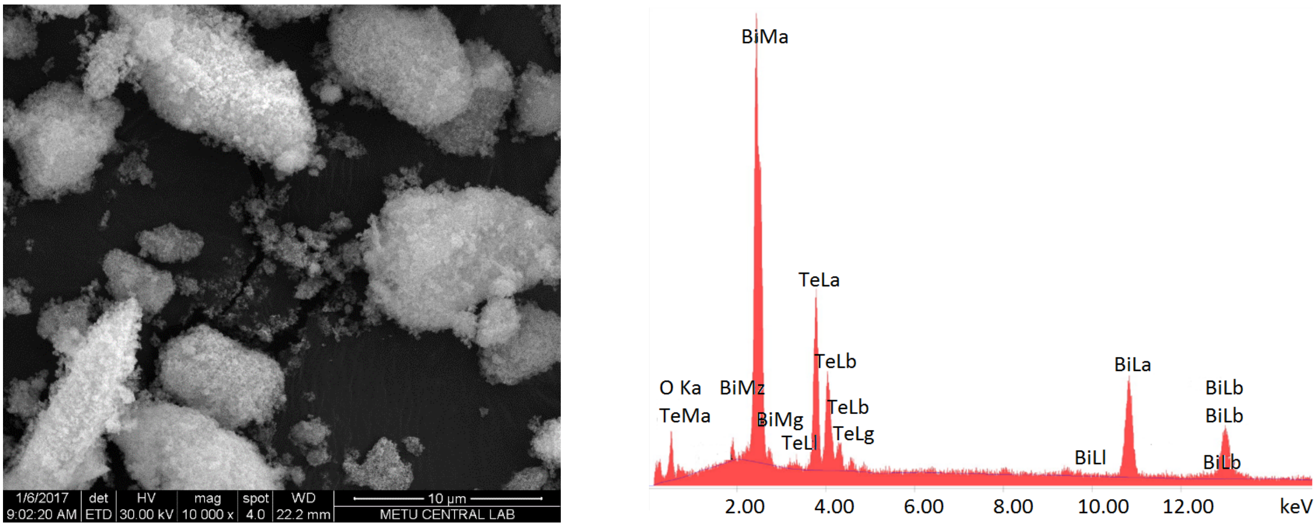

(a) (b)

Figure 4. SEM image and EDAX spectrum of Bi_2Te_3 nanostructure.

The AFM studies revels that the atom arrangement of the nanostructure is in homogenous. Figure 5 provide the 3D view of of Bi_2Te_3 nanostructure. In this figure it is conform that the structure in nano crystalline in form [32]. The roughness parameter also observed through this figure. In our observation the average roughness value is about ~68 nm. The results of this investigation are significant because large position noise in a nano positioner can obscure an AFM's surface roughness measurement.

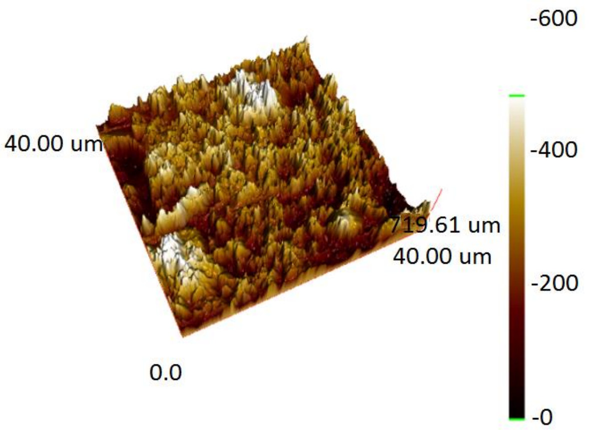

Roughness Parameters	
Coefficient	Value
Average (Ra)	68.06 nm
Root Mean Squre (Rq)	86.98 nm
Skewness (Rsk)	0.310
Kurtosis (Rku)	3.566
Maximum (Rp)	719.61 nm
Minimum (Rv)	0.00 nm
Peak To Peak (Rt)	719.61 nm
Ten Point Height (Rz)	698.21 nm

Figure 5. AFM image of Bi_2Te_3 nanostructure.

Figure 6 shows the TEM micrograph of Bi_2Te_3 nanostructure that exhibit an aggregate phenomenon, and the primary crystalline size is about low dimension. The mean crystalline size is distribution is quite narrow. But, when the nanostructures is smaller, the wavelength of the electrons is closer to the range of the particle sizes. The laws of classical physics must be substituted by quantum confinement or quantum size effect [33].

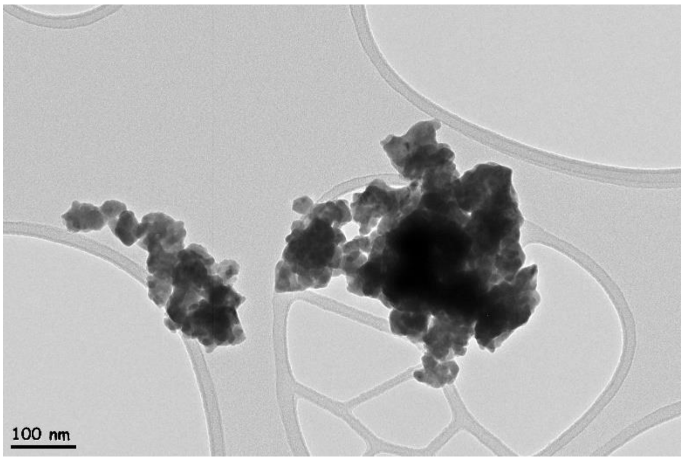

Figure 6. TEM micrograph of Bi_2Te_3 nanostructure.

4. Conclusion

In summary, the experimental results revealed the sample exhibits the nanostructure form of low dimension. The characterizing aspects a simple two–step co–precipitation chemical solution route has the satisfactory for developing the Bi_2Te_3 nanostructure. In conclusion, using this procedure may open a way for exploring high-performance TE materials that can be easily applicable to TE applications.

Acknowledgements

This research work was supported by Scientific Research Project Office of Manisa Celal Bayar University (No: 2016-147). This study was also presented as invited speakers at the 2nd International Scientific and Vocational Studies Congress (BILMES 2018, Urgup, Nevsehir, Turkey).

References

[1] S. Chen, Y, Hutabalian, S. Lu, Y. Peng and Y. Lin. "Interfacial reactions in In/Bi_2Se_3, In/Bi_2Te_3 and In/$Bi_2(Se_{.02}Te_{.08})_3$ couples." J. Alloys and Compounds 779 (2019) 347–359.
[2] P. Khade, T. Bagwaiya, S. Bhattacharya, S. Rayaprol, A.K. Sahu and V. Shelke. "Transport properties of bismuth telluride compound prepared by mechanical alloying." AIP Conference Proceedings 1832 (2017) 110015.
[3] C. Sudarshan, S. Jayakumar, K. Vaideki and C. Sudakar. "Effect of vacuum annealing on structural, electrical and thermal properties of e-beam evaporated Bi_2Te_3 thin films." Thin Solid Films 629 (2017) 28–38.
[4] M.R. Burton, S.J. Richardson, P.A. Staniec, N.J. Terrill, J.M. Elliott, A.M. Squires, N.M. White and Iris S. Nandhakumar. "A novel route to nanostructured bismuth telluride films by electrodeposition." Electrochemistry Communications 76 (2017) 71–74.
[5] D. Merten, K.T. Kallis, F.J. Giebel, J. Zimmermann, R.P. Poloczek, H.L. Fiedler and P. Lilienthal. "Lithography independent nanostructuring of Bi_2Te_3 thermoelectric devices." 14th IEEE India Council International Conference, IEEE (2017) 1–4.
[6] Z. Chai, X. Hu, Y. Zhao, Y. Wu, S. Wang, H. Yang and Q. Gong. "Structural surface wave properties of amorphous Bi_2Te_3 by pulsed laser deposition in the visible and near-infrared regions." AIP Advances 8(6) (2018) 065324.
[7] C. Lei, Karl S. Ryder, E. Koukharenko, M. Burton, and Iris S. Nandhakumar. "Electrochemical deposition of bismuth telluride thick layers onto nickel." Electrochemistry Communications 66 (2016) 1–4.
[8] K. Ahn, J.K. Won, Y.K. Kang, C. Hwang, I. Chung and M.G. Kim. "Thermoelectric properties of nano-bulk bismuth telluride prepared with spark plasma sintered nano-plates." Current Applied Physics 19(2) (2019) 97–101.
[9] H. Mamur, O. F. Dilmac, H. Korucu and M.R.A. Bhuiyan. "Cost-effective chemical solution synthesis of bismuth telluride nanostructure for thermoelectric applications." Micro & Nano Letters (2018).
[10] M.M. Rashad, A. El-Dissouky, H.M. Soliman, A.M. Elseman, H.M. Refaat and A. Ebrahim. "Structure evaluation of bismuth telluride (Bi_2Te_3) nanoparticles with enhanced Seebeck coefficient and low thermal conductivity." Materials Research Innovations 22(6) (2018) 315–323.
[11] F.H. Lin, and C.J. Liu. "A simple energy-saving aqueous synthesis of Bi_2Te_3 nanocomposites yielding relatively high thermoelectric power factors." Ceramics International in press (2018).
[12] N.S. Abishek, and K.G. Naik, "Influence of gamma ray irradiation on stoichiometry of hydrothermally synthesized bismuth telluride nanoparticles." AIP Conference Proceedings 1953(1) (2018) 030067.

[13] C. Kim, D.H. Kim, Y.S. Han, J.S. Chung, S. Park, H. Kim, "Fabrication of bismuth telluride nanoparticles using a chemical synthetic process and their thermoelectric evaluations." Powder technology 214(3) (2011) 463–468.

[14] Y.Q. Cao, T.J. Zhu, X.B. Zhao, "Thermoelectric Bi_2Te_3 nanotubes synthesized by low temperature aqueous chemical method." J. Alloys and Comps. 449 (2008) 109–112.

[15] Y. Liu, Q. Wang, J. Pan, Y. Sun, L. Zhang, and S. Song, "Hierarchical Bi_2Te_3 Nanostrings: Green Synthesis and Their Thermoelectric Properties." Chemistry–A European Journal, 24(39) (2018) 9765–9768.

[16] S.L. Morelhao, C.I. Fornari, P.H. Rappl, and E. Abramof. "Nanoscale characterization of bismuth telluride epitaxial layers by advanced X-ray analysis." J. Applied Crystallography 50(2) (2017) 399–410.

[17] T. Sharifi, S. Yazdi, G. Costin, A. Apte, G. Coulter, C. Tiwary and P.M. Ajayan. "Impurity-Controlled Crystal Growth in Low-Dimensional Bismuth Telluride." Chemistry of Materials 30(17) (2018) 6108–6115.

[18] M. Mahvi, H. Delavari, and R. Poursalehi. "Rapid microwave-assisted synthesis of Bi_2Te_3 nanoflakes as an efficient contrast agent for X-ray computed tomography." Ceramics International 44(8) (2018) 9679–9683.

[19] J. Yang, J. He and S. ZhangJanuary. "Bi_2Te_3 Nanorods: Preparation, Reaction Mechanism and Electrochemical Property." IOP Conference Series: Materials Science and Engineering 201(1) (2018) 012011.

[20] A. Danine, K. Termentzidis, S. Schaefer, S. Li, W. Ensinger, C. Boulanger, D. Lacroix, and N. Stein, "Synthesis of bismuth telluride nanotubes and their simulated thermal properties." Superlattices and Microstructures 122 (2018) 587–595.

[21] M.R.A. Bhuiyan and H. Mamur. "Review of the bismuth telluride (Bi_2Te_3) nanoparticle: growth and characterization" International J. Energy Applications and Technologies 3(2) (2016) 27–31.

[22] H. Mamur, M.R.A. Bhuiyan, F. Korkmaz and M. Nil. "A review on bismuth telluride (Bi_2Te_3) nanostructure for thermoelectric applications." Renewable and Sustainable Energy Reviews 82(3) (2018) 4159-4169.

[23] M.M. Rashad, A. El-Dissouky, H.M. Soliman, A.M. Elseman, H.M. Refaat, and A. Ebrahim. "Structure evaluation of bismuth telluride (Bi_2Te_3) nanoparticles with enhanced Seebeck coefficient and low thermal conductivity." Materials Research Innovations 22(6) (2018) 315–323.

[24] G. Zhang, B. Kirk, L.A. Jauregui, H. Yang, X. Xu, Y.P. Chen and Y. Wu. "Rational synthesis of ultrathin n-type Bi_2Te_3 nanowires with enhanced thermoelectric properties." Nano letters 12(1) (2011) 56–60.

[25] A.M. Elseman, A.E. Shalan, M.M. Rashad, A.M. Hassan, N.M. Ibrahim and A.M.Nassar. "Easily attainable new approach to mass yield ferrocenyl Schiff base and different metal complexes of ferrocenyl Schiff base through convenient ultrasonication-solvothermal method." J. Phys. Organic Chem. 30(6) (2017) 1–10.

[26] M.M. Rashad, A.M. Hassan, A.M. Nassar et al. "A new nano-structured Ni(II) Schiff base complex: synthesis, characterization, optical band gaps, and biological activity." Appl. Phys. A 117(2) (2014) 877–890.

[27] J. Gooth, R. Zierold, P. Sergelius et al. "Local magnetic suppression of topological surface states in Bi_2Te_3 nanowires." ACS Nano. 10(7) (2016) 7180–7188.

[28] P. Srivastava, K. Singh. "Effects of Cs-doping on morphological, optical and electrical properties of Bi_2Te_3 nanostructures." Mater. Lett. 136 (2014) 337–340.

[29] J. Fu, S. Song, X. Zhang, F. Cao, L. Zhou, X. Li, H. Zhang. "Bi_2Te_3 nanoplates and nanoflowers: synthesized by hydrothermal process and their enhanced thermoelectric properties." Cryst. Engg. Comm. 14(6) (2012) 2159–2165.

[30] S. Li, S. Zhang, Z. He, M. Toprak, C. Stiewe, M. Muhammed and E. Müller. "Novel solution route synthesis of low thermal conductivity nanostructure bismuth telluride." J. Nanoscience and Nanotech. 10(11) (2010) 7658–7662.

[31] S.L. Benjamin, C.H. de Groot, C. Gurnani, A.L. Hector, R. Huang, E. Koukharenko, W. Levason and G. Reid. "Controlling the nanostructure of bismuth telluride by selective chemical vapour deposition from a single source precursor." J. Mater. Chem. A 2(14) (2014) 4865–4869.

[32] H. Huang, W.L. Luan and S.T. Tu. "Influence of annealing on thermoelectric properties of bismuth telluride films grown via radio frequency magnetron sputtering." Thin Solid Films 517(13) (2009) 3731–3734.

[33] M.R. Dirmyer, J. Martin, G.S. Nolas, A. Sen, J.V. Badding. "Thermal and electrical conductivity of size-tuned bismuth telluride nanoparticles." Small 5(8) (2009) 933–937.